Mon. Not. R. Astron. Soc. **000**, 000–000 (0000) Printed 29 March 2010 (MN LATEX style file v2.2)

Measuring cosmic magnetic fields by rotation measure-galaxy cross-correlations in cosmological simulations

F. Stasyszyn[1⋆], S. E. Nuza[1], K. Dolag[1], R. Beck[2] and J. Donnert[1]

[1] *Max-Planck-Institut für Astrophysik, Karl-Schwarschild Str. 1, D85748, Garching, Germany*
[2] *Max-Planck-Institut für Radioastronomie, Auf dem Hügel 69, 53121, Bonn, Germany*

Accepted. Received; in original form

ABSTRACT

Using cosmological MHD simulations of the magnetic field in galaxy clusters and filaments we evaluate the possibility to infer the magnetic field strength in filaments by measuring cross-correlation functions between Faraday Rotation Measures (RM) and the galaxy density field. We also test the reliability of recent estimates considering the problem of data quality and Galactic foreground (GF) removal in current datasets. Besides the two self-consistent simulations of cosmological magnetic fields based on primordial seed fields and galactic outflows analyzed here, we also explore a larger range of models scaling up the resulting magnetic fields of one of the simulations. We find that, if an unnormalized estimator for the cross-correlation functions and a GF removal procedure is used, the detectability of the cosmological signal is only possible for future instruments (e.g. SKA and ASKAP). However, mapping of the observed RM signal to the underlying magnetization of the Universe (both in space and time) is an extremely challenging task which is limited by the ambiguities of our model parameters, as well as to the weak response of the RM signal in low density environments. Therefore, we conclude that current data cannot constrain the amplitude and distribution of magnetic fields within the large scale structure and a detailed theoretical understanding of the build up and distribution of magnetic fields within the Universe will be needed for the interpretation of future observations.

Key words: (magnetohydrodynamics) MHD - magnetic fields - methods: numerical - galaxies: clusters

1 INTRODUCTION

Magnetic fields in the Universe are found in almost all studied environments. In particular, their presence in the inter-galactic medium (IGM; see Beck 2009, for a recent review) and in the intra-cluster medium (ICM) is confirmed by diffuse radio emission as well as by observations of Faraday Rotation Measures (RM) towards polarized radio sources within or behind the magnetized medium (e.g. Govoni 2006). On the largest scales, like those of filaments, magnetic fields are notoriously difficult to measure and available data is still incomplete. This is especially difficult because these measurements require either a high thermal density (for RMs) or the presence of relativistic particles (for the synchrotron emission). Therefore, measurements of the magnetic field strength have been successfull for high density regions of collapsed objects (e.g. galaxies and galaxy clusters), and thus, fields significantly below the μG level can hardly be detected.

Recently an interesting attempt to constrain the value of large scale cosmic magnetic fields was done by Lee et al. (2009). These authors detected a positive cross-correlation signal between the galaxy distribution in the SDSS Sixth Data Release (Adelman-McCarthy et al. 2008) and the RM values extracted from the Taylor et al. (2009) catalog. Using the amplitude of this signal, together with a simplified model for the magnetic fields configuration in the Universe (estimated from its mean electron density), and computing the RM typical values expected from this coherent field in a given length scale, they were able to derive limits for the corresponding cosmic magnetic fields.

In this work, we want to investigate: (*i*) to what extent a self-consistent treatment of the cosmological RM signal based on magneto-hydrodynamical (MHD) simulations of structure formation changes the expected shape and amplitude of such a correlation signal, and (*ii*) how such an approach is affected by the presence of the Galactic foreground (GF) and noise in the final RM signal. Both points are of extreme importance, if robust field properties are to be derived from any observed signal. Furthermore, the appearance of magnetic field reversals (as observed in galaxy clusters at various length scales) will alter the cosmological signal magnitude and shape, whereas the residuals of any foreground and measurement errors will bias the relation between the amplitude of the corre-

⋆ E-mail: fstasys@mpa-garching.mpg.de

lation function and the underlying cosmological field. In order to self-consistently treat the cosmic magnetic fields, we make use of several cosmological MHD simulations which compute the resulting magnetization of the cosmological structures (e.g. amplitude and structure) following different models for the origin and seeding process of such magnetic fields. We also construct magnetic field models with much higher magnetization amplitude in the low density regions to test how the resulting signatures of more extreme models affect our results. Here we scale up the predicted amplitude of the magnetic field in filaments by several orders of magnitude to test if such strong magnetic fields in low density regions significantly effect the expected correlation signal. By introducing GF and adding noise to the signal on top of the underlying cosmological signal, we can study how the shape and amplitude of the cross-correlation function would be modified when considering actual observations. To avoid further complications we ignore the cosmological evolution of magnetic fields, which, in principle, would be consistently treated within our cosmological MHD simulations. Hence, we neglect the evolution of the cosmic magnetic field seen in the simulation as a result of the structure formation process, and assume the present day magnetization of the simulated universe to be present up to the redshift of the sources.

The paper is organized as follows. In Section 2 we describe the cosmological MHD simulations used and how we compute the synthetic RM catalogs. In Section 3 we discuss the cross-correlation estimators used, the estimation of the intrinsic uncertainties due to the limited number of lines of sight probing the magnetization of the cosmological structures, the different signals expected for the various magnetization of the universe, as well as the uncertainties induced by the redshift distribution of the sources. In Section 4 we show how the shape and amplitude of the signal is affected by the recipe normally used to remove the foreground signal, due to observational noise and to the Galaxy itself. In Section 5 we summarize the combination of all the effects, and present the resulting observable signal of the different magnetic field models. Finally, our conclusions are given in Section 6.

2 THE SIMULATIONS

2.1 The cosmological MHD simulations

We used results from one of the constrained, cosmological MHD simulations presented in Dolag et al. (2005) and Donnert et al. (2009). In both simulations, the initial conditions for a constrained realization of the local Universe were the same as used in Mathis et al. (2002). The initial conditions were obtained based on the the *IRAS* 1.2-Jy galaxy survey (see Dolag et al. 2005, for more details). Its density field was smoothed on a scale of $7\,\mathrm{Mpc}$, evolved back in time to $z = 50$ using the Zeldovich approximation, and used as an Gaussian constraint (Hoffman & Ribak 1991) for an otherwise random realization of a ΛCDM cosmology ($\Omega_M = 0.3$, $\Lambda = 0.7$, $h = 0.7$). The *IRAS* observations constrain a volume of $\approx 115\,\mathrm{Mpc}$ centered on the Milky Way. In the evolved density field, many locally observed galaxy clusters can be identified by position and mass. The original initial conditions were extended to include gas by splitting dark matter particles into gas and dark matter, obtaining particles of masses $6.9 \times 10^8\ \mathrm{M}_\odot$ and $4.4 \times 10^9\ \mathrm{M}_\odot$ respectively. The gravitational softening length was set to $10\,\mathrm{kpc}$.

The magnetic field was followed by our MHD simulations through the turbulent amplification driven by the structure formation process. For the magnetic seed fields, the first simulation (labeled *MHD*) followed a cosmological seed field (see Fig. 1), while

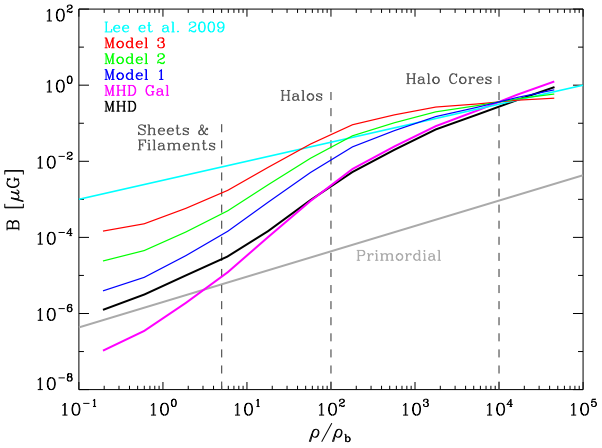

Figure 1. Mean cosmic magnetic field as a function of density (in units of the mean cosmic baryon density) obtained from two, fully self-consistent, cosmological MHD simulations for different magnetic field origins (*MHD* and *MHD Gal*), as well as three models, where we artificially scaled-up the magnetic field intensity at low densities to obtain scenarios with extreme values in filaments (*Model 1*, *Model 2* and *Model 3*). For more details on these models see the text. Additionally, the primordial seed fields of the *MHD* simulation and that obtained by Lee et al. (2009) are shown.

in the second (labeled *MHD Gal*) we used a semi-analytic model for galactic winds. In particular, we considered the result of the *0.1 Dipole* simulation from Donnert et al. (2009). In both simulations, the resulting magnetic field at $z = 0$ reproduce the observed Rotation Measure in galaxy clusters very well. A visual impression for the magnetic field within the two different simulations and their corresponding galaxy distribution is shown in Fig. 2.

2.2 Artificial MHD models

As is clearly visible in Fig. 2, such cosmological simulations usually predict relatively low magnetic fields in low density regions. To explore more extreme models, we scaled up the magnetic field of the *MHD* simulation by a factor

$$B_{1,2,3} = B_{\mathrm{MHD}} \times \left(\frac{\rho}{\rho_{\mathrm{scale}}}\right)^{\alpha}, \qquad (1)$$

with α being 1/3 (*Model 1*), 1/2 (*Model 2*) and 2/3 (*Model 3*). Here ρ_{scale} denotes density scale for fixing the magnetic field, which we choose to be 10^4 times the mean cosmic baryon density. The resulting behaviour of the mean magnetic field as a function of baryon density for the original runs, as well as for the scaled-up models, are shown in Fig. 1. Note that the lines shown reflect the mean value of the magnetic field at the corresponding overdensity, while the dispersion of its amplitude can span several orders of magnitude in each density bin (see Dolag et al. 2005). We want to stress that such scaled-up magnetic fields are artificial models, as the primordial field needed to generate them would be well above current cosmological constraints (e.g. from CMB). Such strong seed fields would lead to an overprediction of the magnetic field amplitude in galaxy clusters by the simulations and it is quite unclear which physical process could be responsible to avoid this. We also remark that the scaled-up models lead to slightly lower central values for the magnetic field inside of galaxy clusters. This is qualitative in agreement with what is needed to fit the observed RM signal within the Coma galaxy cluster (see Bonafede et al. 2010).

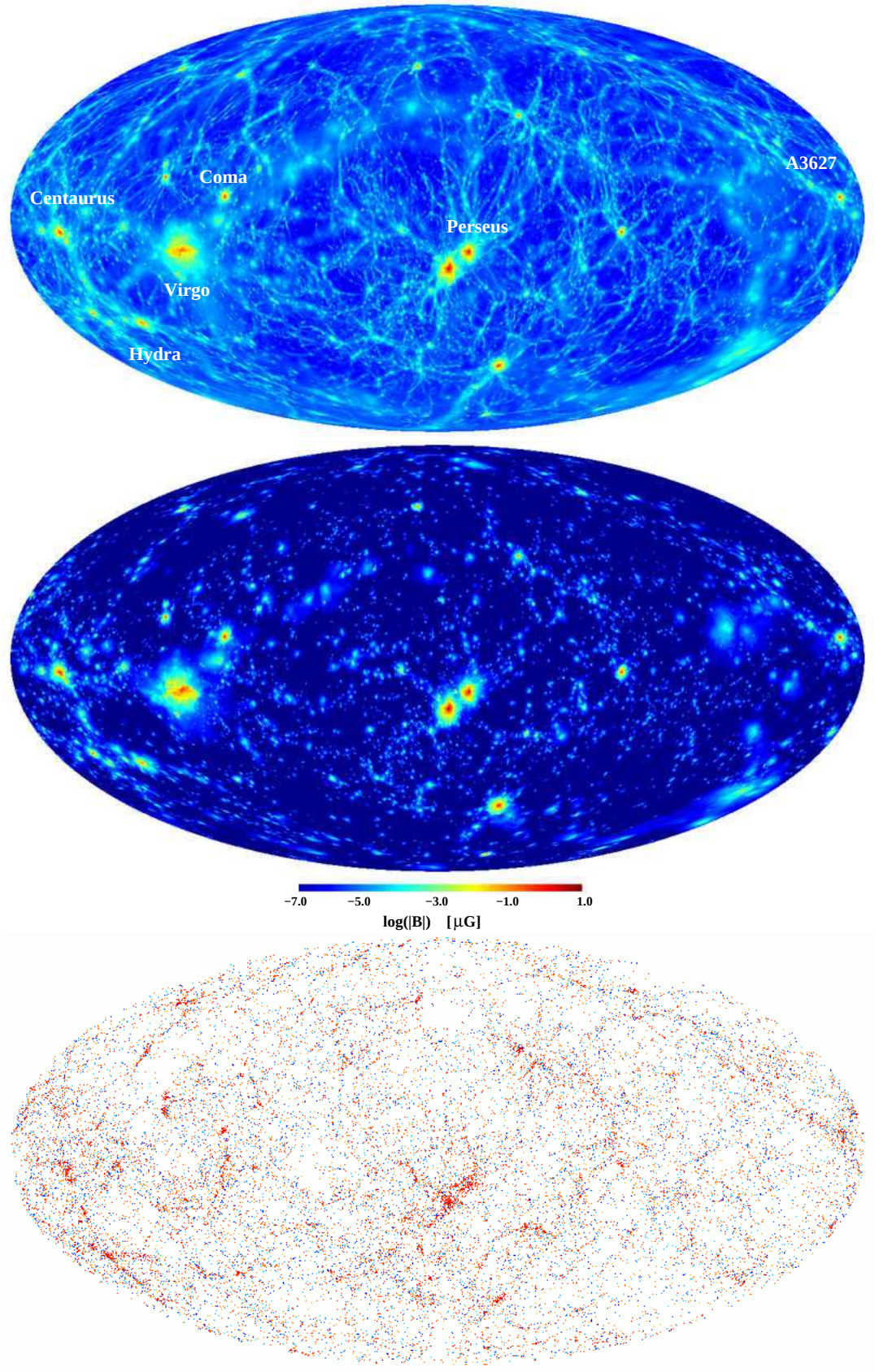

Figure 2. Full sky maps of the local universe in supergalactic coordinates for the projected magnetic field in the *MHD* run (upper panel) and in the *MHD Gal* run (middle panel). The galaxy distribution expected from the corresponding hydrodynamical run is shown in the bottom panel. Galaxies are colour-coded from blue to red using their $B-V$ colours ($0.3 < B-V < 1$; see Nuza et al. 2010).

Table 1. Mean and standard deviations of RM absolute values for the different catalogs at $z = 0.03$ and estimates for $z = 0.52$ and $z = 1.03$. The catalogs were constructed in each case using four different realizations (see text). *MHD* is our fiducial structure formation model. *Models 1, 2* and *3* are its scaled-up versions. *MHD Gal* includes a semi-analytic model for Galactic winds to seed magnetic fields at $z = 4.1$.

Model	$\overline{\lvert\mathrm{RM}\rvert}_{z=0.03}$ [rad m^{-2}]	$\Delta\overline{\lvert\mathrm{RM}\rvert}_{z=0.03}$ [rad m^{-2}]	$\overline{\lvert\mathrm{RM}\rvert}_{z=0.52}$ [rad m^{-2}]	$\Delta\overline{\lvert\mathrm{RM}\rvert}_{z=0.52}$ [rad m^{-2}]	$\overline{\lvert\mathrm{RM}\rvert}_{z=1.03}$ [rad m^{-2}]	$\Delta\overline{\lvert\mathrm{RM}\rvert}_{z=1.03}$ [rad m^{-2}]
MHD Gal	0.025	0.010	0.12	0.05	0.21	0.09
MHD	0.018	0.010	0.09	0.05	0.15	0.09
Model 1	0.018	0.008	0.09	0.04	0.15	0.07
Model 2	0.025	0.010	0.12	0.05	0.21	0.09
Model 3	0.040	0.013	0.20	0.06	0.34	0.11

2.3 Synthetic RM catalogs

For each of the 5 models, we construct full sky RM catalogs, sampling the whole sky using 3072 different lines of sight (i.e. $\sim 3^\circ$ resolution) making use of the HEALPix (Górski et al. 2005) tessellation of the sphere. Therefore, our RM catalog contains roughly half as many number of lines of sight to probe the RM signal of the large scale structure than the catalog used as Lee et al. (2009).

Although we are only reproducing much shorter lines of sight than expected in the real Universe (due to the limited volume of the underlying simulation) we believe that the region probed reflects a fair representation of the present large scale distribution of galaxies (Nuza et al. 2010), and therefore, we do not expect the amplitude of any normalized correlation signal to be strongly affected by a lack of fluctuation power.

2.4 Magnetic depth of the universe

On its way to the observer, the polarized radio emission of the observed sources will pass several times through the cosmological filamentary structures. The final RM value does accumulates in a random walk. Examples of the magnetic field structure along some lines of sight through the simulated local universe can be found in previous work (e.g. Dolag et al. 2005, Fig. 12; Dolag et al. 2009, Fig. 10). The magnitude of the observed RMs, and thus, the mean of the RM absolute values, will strongly depend on the *magnetic depth* (given by the redshift range probed) accessible to the observed sample of radio sources. In addition, if the magnetic field changes during the formation of the universe, such changes have to be convolved with the redshift distribution of the observed sources. For simplicity, we assume that the magnetization of the universe at the time of interest was the same as today and that all sources towards the RMs are measured at the same redshift, e.g. all lines of sight used probe the same *magnetic depth* of the universe.

Unfortunately, our cosmological MHD simulation is much smaller than is required to compare with observations directly and therefore we have to extrapolate our calculated RMs to the redshift of the real observed sources. With the size of our simulation box, we can probe only out to $z = 0.03$. Because of this, we account for the increase of the RM values due to a random walk process towards higher redshift by assuming the same contribution of cosmic structures to estimate the cosmological RMs. This is done by replicating the original volume 15 and 22 times (corresponding to redshifts out to $z = 0.52$ and $z = 1.03$). As shown in Table 1, the associated RM amplification factors, including the shift of the rest-frame frequencies due to the cosmological expansion for each replication of the box, are 4.97 and 8.54 respectively. We will use such expected amplified RM signals in the following analysis, indicating this by adding the redshift used for the *magnetic depth* together with the model name. Note that to increase the RM signal by a factor of 100 one must probe cosmic structures up to $z \approx 8$.

Even for the extreme scaled-up models and extrapolation out to $z = 1.03$, the expected RM signal is still one order of magnitude smaller than the reported value by Lee et al. (2009) in their simplified model (i.e. $|\mathrm{RM}| \approx 2$ rad m^{-2}). This emphasizes the fact that simulations that properly take the cosmological structures into account are needed to relate any possible correlation signal to global magnetic field values. Note also that such small signals are expected to be very sensitive to measurement errors which will scale with the even much larger foreground signal imposed by our galaxy. We explore these problems in the following sections.

3 EVALUATING THE COSMOLOGICAL CROSS-CORRELATION SIGNAL

3.1 Estimators

We compute the cross-correlation signal between the RM computed along 3072 lines of sight using a HEALPix tessellation of the sky and the angular positions of simulated galaxies. For every direction, we count the number of galaxies lying at an angle between θ and $\theta + d\theta$, weighting the counts with the corresponding absolute RM value. Formally, the cross-correlation function between $|\mathrm{RM}|$ and the galaxy density n is defined as follows

$$\omega_{\mathrm{RM}}(\theta) \equiv \frac{\langle \Delta n(\theta) |\mathrm{RM}| \rangle}{\bar{n}\overline{|\mathrm{RM}|}}, \tag{2}$$

where Δn measures the fluctuations around the mean value of n, $\bar{n}$ is the mean density of the galaxy sample, $\overline{|\mathrm{RM}|}$ is the mean of the $|\mathrm{RM}|$ catalog, and $\langle \ldots \rangle$ denotes ensemble average. If the distributions of n and RM are Gaussian, this estimator is insensitive to the addition of an uncorrelated signal (like noise and/or foreground). While for the galaxy density n a Gaussian distribution is still a reasonable assumption, the RM absolute values are strongly non-Gaussian. Therefore, it cannot be easily predicted how this estimator will behave once the observational process is included. In fact, Lee et al. (2009) used a different estimator, where the normalization by $\overline{|\mathrm{RM}|}$ is not evaluated, i.e.

$$\xi_{\mathrm{RM}}(\theta) \equiv \frac{\langle \Delta n(\theta) |\mathrm{RM}| \rangle}{\bar{n}}. \tag{3}$$

Note that this estimator is likely quite sensitive to processes which

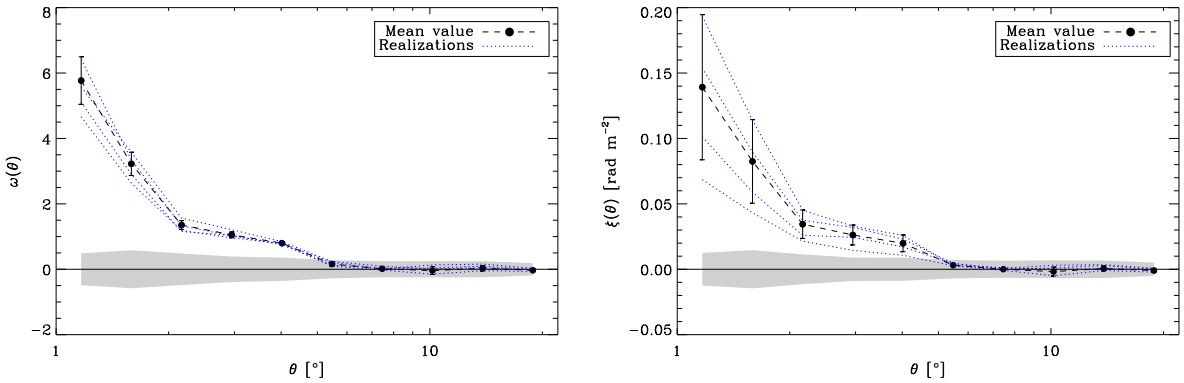

Figure 3. Angular cross-correlation functions, for the full sky map based on the original *MHD Gal* simulation, using the two estimators presented in the text (see Eqs. 2 and 3). In both panels, the results of different magnetic field realizations can be seen as blue dotted lines. The average result is shown as black filled circles. Error bars denote the 1-σ dispersion due to the different realizations. The grey area indicates the *null* signal obtained by reshuffling the RMs.

change the value of $\overline{|\mathrm{RM}|}$, such as the *magnetic depth* probed by the redshift distribution of the sources.

3.2 Evaluating uncertainties

We investigate two kind of errors for our simulated cross-correlation functions. To estimate the significance of our obtained correlation signal, we randomly shuffled the RM data twenty times. This allow us to take into account the variance given by the used sampling and reveals the significance of the correlation itself. We will indicate this as the expected level for a *null* signal in the figures. A second source of errors is given by the magnetic field realizations available inside the simulated volume. Since we are still using a small number of RM points (i.e. 3072), this also introduces significant noise to the correlation functions obtained. It is beyond the scope of the present work to produce several independent simulations based on different realizations of the initial magnetic seed field. Therefore, we assesed this by calculating the RM signal of each particle using either the x, y and z component or the radially projected magnetic field component. Note that the first three components are only statistically equivalent to the radially projected component once a isotropic distribution of the magnetic field is assumed. Next we use these four realizations of the RM signal to estimate the uncertainty according to the underlying cosmic magnetic field realization in the simulations. This uncertainty is then added as error bars to the individual models.

Fig. 3 shows the correlation function signal obtained from the *MHD Gal* model for the two estimators (ω_{RM} and ξ_{RM}). It shows the individual signal for the four different realizations of the magnetic fields and the resulting mean signal with their corresponding error bars. The *null* signal obtained from reshuffling the RMs twenty times is indicated by the grey area. Whereas the uncertainties coming from the magnetic field variance in the different realizations changes the amplitude of $\omega_{RM}(\theta)$ only by 10%, it is clearly visible that using the unnormalized $\xi_{RM}(\theta)$ estimator introduces much larger uncertainties in its amplitude (by roughly a factor ~ 2). It also highlights the fact that using this estimator together with the mean of the $|\mathrm{RM}|$ signal to infer the underlying magnetic field will generate large uncertainties in the estimation. It is important to keep in mind that the ratio between both estimators (in every scale) for each of the individual realizations is given by the mean value of the corresponding absolute RMs. However, the normalization of the different realizations of each magnetic field model can vary significantly (up to a factor of ~ 3). Whereas in the normalized cross-correlation this is naturally absorbed, in the unnormalized case it enters in the error bars when building the assembly average over different realizations.

As a final remark, we expect that both errors will decrease similarly as Poissonian errors do when the number of lines of sight to probe the RM signal is increased.

3.3 Magnetic depths

As mentioned before, to correctly interpret the cross-correlation signal we must consider the *magnetic depth* probed by the RMs. Fig. 4 shows the expected signal, assuming a non-evolving magnetic field probed by the sources up to a certain given redshift. As expected, the normalized correlation function signal $\omega_{RM}(\theta)$ is insensitive to the particular probed volume and its amplitude reflects the underlying magnetic field distribution, independent on the redshift distribution of the sources. On the other hand, the signal given by the unnormalized estimator $\xi_{RM}(\theta)$ increases as a function of the *magnetic depth* as expected. In this case, the amplitude changes by more than a factor of two if the redshift distribution of the radio sources is changed from $z = 0.52$ to $z = 1.03$. This means that one has to consider the redshift distribution of the radio sources towards the observed RMs in order to relate the amplitude of the signal to the underlying magnetization of the large scale structures. Therefore, it is difficult to interpret such an observed signal (as done e.g. by Lee et al. 2009).

3.4 Magnetic field models

Fig. 5 shows the cross-correlation function signal obtained from the five different models investigated. The two shaded regions indicate the contribution of the two errors discussed before. The shape and the ordering of the correlation signal of ω_{RM} reflects the scaling of the underlying magnetic field models with density. In particular, the crossover of the correlation function reflects the one seen in the underlying magnetic field models very well (see Fig. 1). The correlation signal thus indeed carries information about the strength and distribution of the cosmic magnetization. It is expected that using more lines of sight will reduce the statistical errors enough to make our extreme models clearly distinguishable. This would be

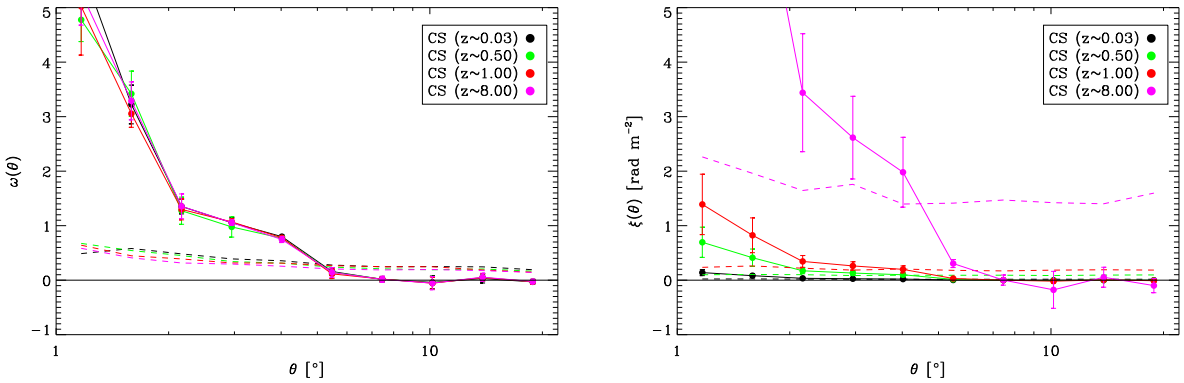

Figure 4. Angular cross-correlation function, based on the original *MHD Gal* cosmological signal (CS), evaluated for different *magnetic depths* probed by the RMs, using the two estimators presented in the text (left and right panels).

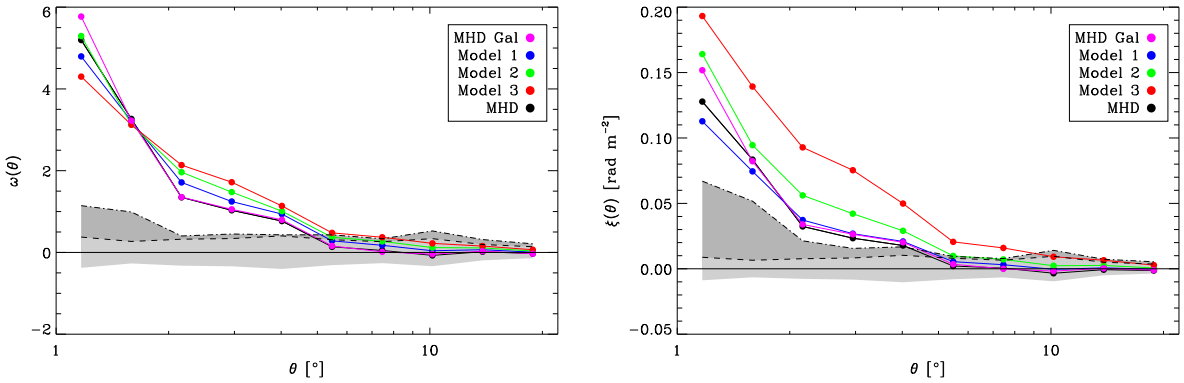

Figure 5. Comparison between the angular cross-correlation functions, for the full sky maps in different models, using the two estimators presented in the text (left and right panels). Black solid line indicates the *MHD* model, while blue, light green and red indicate *Model 1*, *2* and *3* respectively. Pink solid line indicates the *MHD Gal* model. In both panels, the light grey shaded area indicates the randomly shuffled region, while the dark grey area indicates the magnitude of typical errors present at a given scale due to the different RM realizations.

in principle possible with the available number of line of sights in current data (e.g. Taylor et al. 2009).

The unnormalized correlation function ξ_{RM} leads to a larger relative change of the amplitude of the correlation signal for the different magnetic field models, especially for the ones with very high magnetic fields in filaments. However, the resulting signal comes with much larger errors (coming mainly from the different magnetic field realizations in the same models) and is therefore less significant. Also, the ordering of the magnetic field models with less extreme magnetic field values in filaments is not longer reflected in the correlation amplitude, particularly towards smaller impact parameters.

In summary, we conclude that the correlation signal for ω_{RM} inherits a clear signal from the cosmological magnetization, whereas the correlation function ξ_{RM} (as used in Lee et al. 2009) is very difficult to interpret. Because of the missing normalization, changes in the underlying RM distribution (caused by different realizations of the same magnetic field model or the *magnetic depth* probed by the radio sources) are not compensated for.

4 SIMULATING THE OBSERVATIONAL PROCESS

To test for the effects caused by the observational process on the cross-correlation functions it is important to use an underlying scenario which reflects the expected amplitude of the RM signal. Therefore, we use (unless specifically stated) an underlying *magnetic depth* of the universe of $z = 1$.

4.1 Foreground removal procedure

For RM observations, the removal of the foreground imposed by our galaxy (GF) is a major problem. Usually one assumes that the foreground varies on (much) larger scales than the ones of interest and removes the GF by subtracting a smoothed signal from the original data. Here we test how such a removal procedure affects the underlying cosmological signal traced using correlation functions following exactly the same procedure applied in Lee et al. (2009). At every point, we subtract the mean of the RM absolute values within a given radius (excluding the central value). Specifically, we tested three different angular sizes for the removal (i.e. 3°, 6° and 9°). Fig. 6 shows the result of such foreground subtraction technique on the normalized correlation function for the cosmological signal using the normalized estimator ω_{RM}. At small distances, this procedure leads to a significant suppression of the

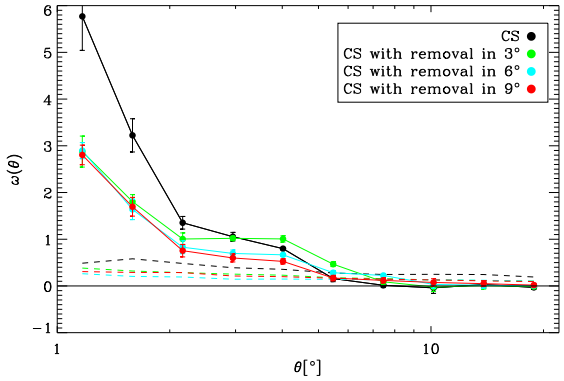

Figure 6. Angular cross-correlation function, based on the *MHD Gal* cosmological signal (CS), assuming a magnetic depth of $z = 0.03$. Shown are the results obtained by subtracting to each $|\mathrm{RM}|$ the average of its neighbors (excluding itself) within a radius of 3°, 6° and 9° for the ω_{RM} estimator.

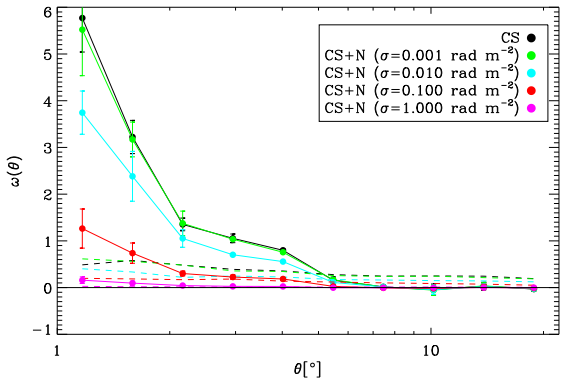

Figure 7. Angular cross-correlation function for the *MHD Gal* cosmological signal (CS) using the ω_{RM} estimator. Same as Fig. 3 (left panel), but including the effects of different random noise (N) scenarios at magnetic depth of $z = 0.03$.

correlation signal, even up to a factor of ~ 2 for angular distances below $\sim 2^\circ$, almost independently of the size of the removing radius. At larger distances, the amplitude of the correlation function is slightly increased (10 – 20%) starting from scales larger than the smoothing radius.

4.2 Adding observational noise

Another problem for the observed RMs are the measurement errors by themselves. For example, since the data recently published by Taylor et al. (2009) is based on only two different frequency bands the resulting RMs will be affected by a significant uncertainty. We also note that these errors are not reduced by the smoothing involved when removing the foreground. The typical error of the observational RMs (as inferred from comparison with a data subset which was observed at more frequency bands) turns out to be around 10 to 20 rad m^{-2} (see Taylor et al. 2009, Fig. 2). In order to estimate the effect of the observational errors, we added random values to our simulated RM signal, which were drawn from a Gaussian distribution with a dispersion given by σ_{RM}. We explored values of 0.001, 0.01, 0.1, 1.0 and 10 rad m^{-2} for σ_{RM}. Note that most of these values are much more optimistic than what is expected from current instruments. However, future instruments, like e.g. SKA and ASKAP will achieve an RM accuracy of a few rad m^{-2} (Beck & Gaensler 2004).

Fig. 7 shows the impact of such measurement errors onto the resulting correlation function. Even $\sigma_{\mathrm{RM}} = 0.01$ (e.g. a hundredth of the actual measurement error) leads to a sizable (ca. 50%) reduction of the correlation signal. Furthermore, $\sigma_{\mathrm{RM}} = 0.1$ (e.g. ten percent of the actual measurement error) reduces the signal by a factor of ~ 5 and $\sigma_{\mathrm{RM}} = 1$ (e.g. nearly the present measurement errors) makes the correlation very close to the one of the corresponding *null* signal. From this it is clear that using the normalized estimator $\omega_{RM}(\theta)$ will be quite problematic. The presence of even small measurement errors (far smaller than what can be reached currently) will affect the shape and amplitude of the correlation function in a way that the information on the cosmic magnetization is basically lost.

4.3 Adding Galactic foreground

In recent years, different models for the Galactic magnetic field were proposed (e.g. Han et al. 2006; Page et al. 2007; Jansson et al. 2008; Sun et al. 2008). To estimate the influence of the GF on the cosmological cross-correlations we produced a synthetic map of the RM signal expected for our galaxy using the publicly available code HAMMURABI (Waelkens et al. 2009), where we made use of the Galactic magnetic model given by Sun et al. (2008). The original model was constructed to give a good representation of the synchrotron emission of the Milky Way but, by missing possible reversals within the model magnetic field, it overproduces the RM signal by a significant factor. We therefore scaled the original model down to obtain a better representation of the observed RMs. We also note that such reversals could lead to significant small scale structures in the RM signal due to the GF, as shown by Sun & Reich (2009). Such fluctuations could significantly compromise the cosmological signal, as they would be present on scales smaller than the one used to filter the GF. However, we do not currently include this effect in our foreground model.

In Fig. 8 we show the obtained RM map models (left column) compared to the observed RM signal (right column) taken from Taylor et al. (2009). From top to bottom we show the original GF model with noise and the RM dataset, a smoothed version of the maps (within 8°), and the residuals when applying the foreground subtraction as described above for 3°. All the synthetic maps are imprinted with an observational error of $\sigma = 10$ rad m^{-2}. The last row shows the synthetic residual map when reducing the noise level to $\sigma = 1$ rad m^{-2} as expected for future instruments. The close-ups show the remaining signal of prominent galaxy clusters in the residual maps. Note that the signal of other prominent clusters, lying behind the Galactic plane, are not longer visible after the foreground subtraction was applied. As expected, when adding such a large, plain foreground signal to the cosmological one, the cross-correlation function vanishes. Therefore, we also applied the GF removal technique described before. The results can be seen in Fig. 9, where the angular cross-correlation function of the combined maps for both estimators is shown. For comparison, we show the expected signal from the plain *MHD Gal* simulation (e.g. assuming a very small *magnetic depth* of $z = 0.03$), the GF signal alone, and the *MHD Gal* combined with the GF signal for a large *magnetic depth* (i.e. $z = 1.03$), as well as for a extreme *magnetic depth* corresponding to $z \approx 8$. In all cases we applied the foreground removal using a radius of 3°. Even for the extreme case of *magnetic depth*, despite the foreground removal applied, the nor-

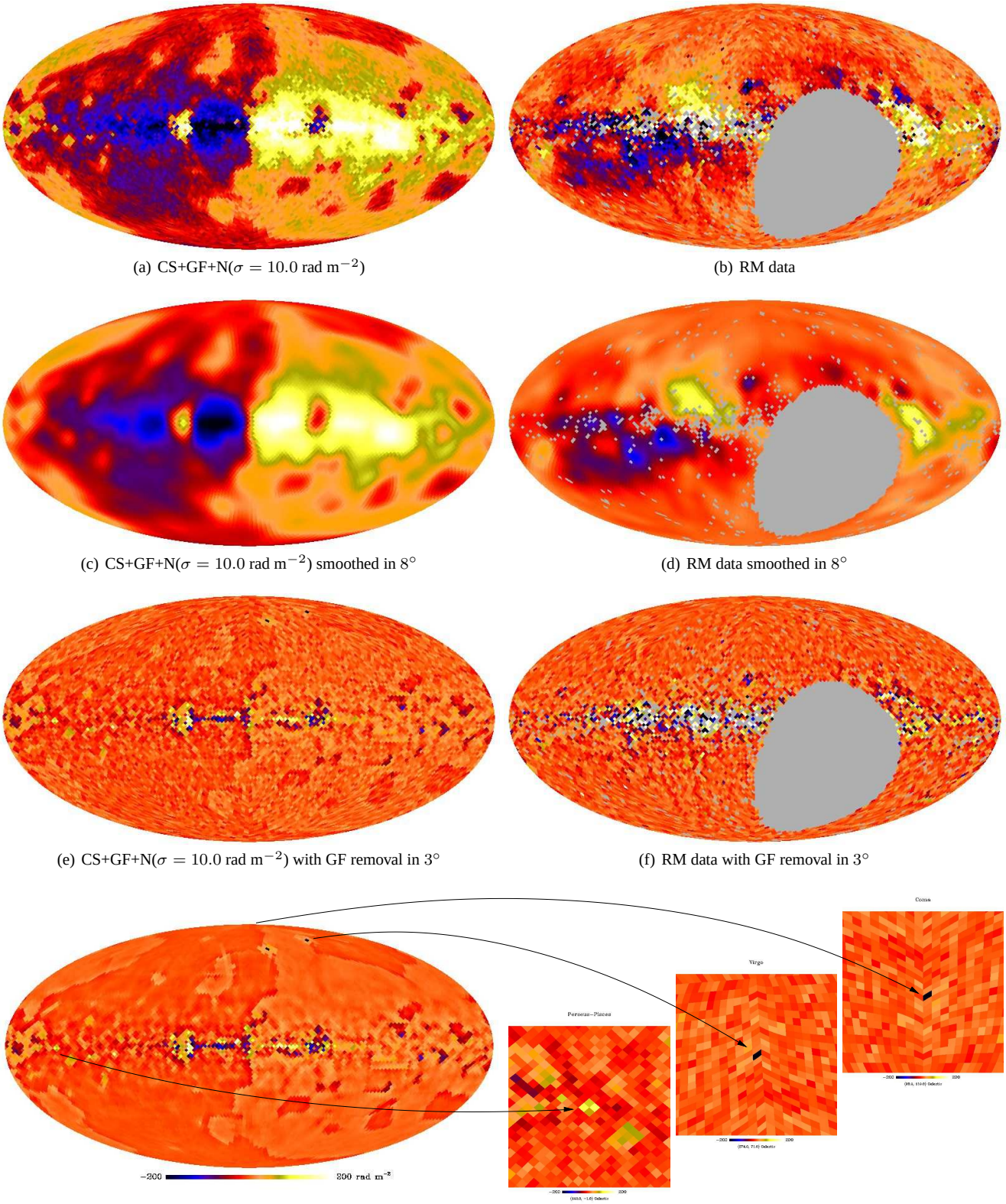

(a) CS+GF+N($\sigma = 10.0$ rad m^{-2})

(b) RM data

(c) CS+GF+N($\sigma = 10.0$ rad m^{-2}) smoothed in 8°

(d) RM data smoothed in 8°

(e) CS+GF+N($\sigma = 10.0$ rad m^{-2}) with GF removal in 3°

(f) RM data with GF removal in 3°

(g) CS+GF+N($\sigma = 1.0$ rad m^{-2}) with GF removal in 3°

Figure 8. Full sky maps in galactic coordinates for the total synthetic signal (left column) and for the observed RMs (right column). The first row shows the Galactic foreground (GF) map generated with the HAMMURABI code of Waelkens et al. (2009) including the cosmological signal (CS) from the *MHD Gal* simulation with a *magnetic depth* of $z = 1$ and an imprinted observational error (N) of $\sigma = 10$ rad m^{-2} compared with the plain RM data given by Taylor et al. (2009). The second row shows the same maps but smoothed by 8° (as in Fig. 4 of Taylor et al. 2009) and the third row shows the resulting residual maps when foreground removal is applied (within 3°). The lower left plot shows the former synthetic map where the noise was reduced to $\sigma = 1$ rad m^{-2}, as it is expected for future observations. In the lower right we show $40^\circ \times 40^\circ$ wide close-ups of three prominent clusters in the simulation (from left to right: Perseus-Pisces, Virgo and Coma).

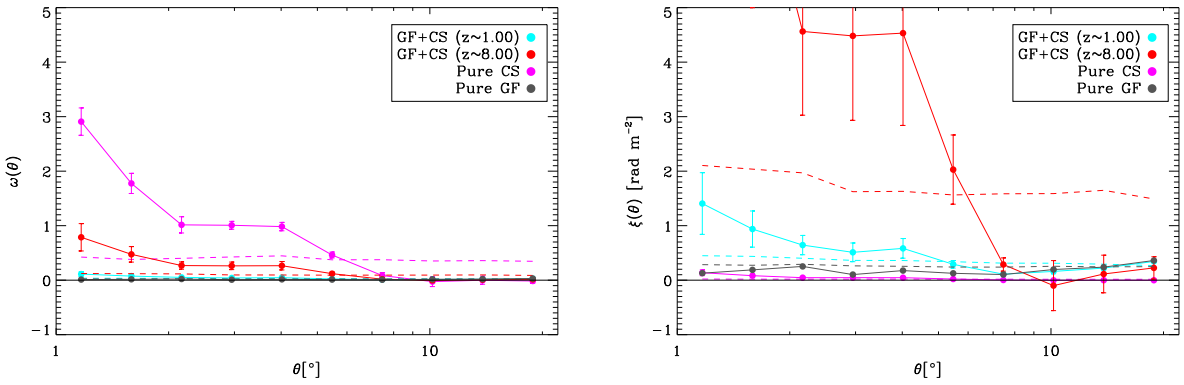

Figure 9. Angular cross-correlation function for the combined cosmological signal (CS) from the *MHD Gal* simulation and the Galactic foreground (GF), including the foreground removal in 3° as described in the text. Shown is the signal using both estimators as presented in the text (see Eqs. 2 and 3).

malized estimator ω_{RM} drops further by a factor of ~ 3 when adding the GF, and drops by a factor of ~ 30 for the most optimistic cosmological signal. On the contrary, the unnormalized estimator ξ_{RM} turns out to be quite insensitive to the foreground provided that the removal technique is applied. The combined signal still corresponds roughly to the original, cosmological one, as can be seen when comparing with Fig. 4.

We conclude, that although the normalized estimator ω_{RM} in principle contains a much more unbiased and reliable imprint of the cosmological magnetization, once GF and observational noise are added, the underlying cosmological signal is completely lost. In constrast, the unnormalized estimator ξ_{RM} is relatively insensitive to the GF and to the noise. However, as seen before, the interpretation of its amplitude and shape is extremely challenging, as it is quite biased by the underlying *magnetic depth* probed by the redshift distribution of the radio sources used in the RM measurements.

5 THE SIMULATED OBSERVATIONAL CROSS-CORRELATIONS: AN EXAMPLE

To study if it is possible to infer the underlying cosmological signal through an observational process which includes GF (and its removal technique) as well as measurement errors by cross-correlating the $|\mathrm{RM}|$ signal with the galaxy density we assume:

- An optimistic *magnetic depth* of the universe of $z = 1.03$;
- A GF according to the model presented in Section 4.3 together with the foreground subtraction technique presented in Section 4.1 using the mean value of the $|\mathrm{RM}|$ map within 3°;
- A measurement error distribution consistent with a Gaussian having $\sigma_{\mathrm{RM}} = 1\,\mathrm{rad\,m^{-2}}$, i.e. a dispersion similar to the magnitude of typical errors achievable by future instruments.

5.1 Piling up the signal

Fig. 10 shows how the resulting signal changes when gradually adding all effects described before, using the *MHD gal* model. As already seen in the individual steps above, the normalized estimator ω_{RM} gives a much more significant signal, but its amplitude and shape suffers dramatically from the inclusion of noise and addition of the GF (despite of the substraction technique applied). On the other hand, the unnormalized estimator ξ_{RM} gives a much less significant signal only mildly changed by all the contributions to the total signal, mainly at larger distances.

5.2 Seeing different cosmic magnetizations

Fig. 11 summarizes the results for such a combination of contributions to the total signal for our five different magnetic field models. The signal for the normalized estimator ω_{RM} (left panel) is reduced by a factor of ~ 50 and the shape does not represent the underlying magnetic field models as well as when applied to the cosmological signal itself (e.g. compare with Fig. 5). The amplitude of the unnormalized estimator ξ_{RM} corresponds to the underlying cosmological signal, but here the original ordering due to the magnetic field models is no longer present. In general, for both estimators, the significance of the total signal is only marginal and the differences between the different magnetic field models lie far inside the error bars. Note that if we would only consider the *null* signal and ignore the errors from the magnetic field realization both estimators would give highly significant detections. The errors coming from the magnetic field realizations are not accessible from the observations and, therefore, the observationally obtained significance of the signal can be misleading unless compared to detailed simulations. As well, both errors can be significantly reduced by using higher number of RMs. The results can also be improved by avoiding the Galactic region (e.g. cutting the region of the maps lying inside $\pm 10^\circ$). In that case, the unnormalized estimator will strongly reduce the power excess seen at distances larger than 3°. Such a cut would also remove the artificial but significant signal seen for separations larger than 10° in both estimators.

6 CONCLUSIONS

Using cosmological MHD simulations of the magnetic field in galaxy clusters and filaments we evaluated the possibility to infer the magnetic field strength in filaments by measuring cross-correlation functions between RMs and the galaxy density field.

We find that the shape of the cross-correlation function using the normalized estimator ω_{RM} (in absence of any noise or foreground signal) nicely reflects the underlying distribution of magnetic field within the large scale structure. However, a very large number of lines of sight probed by RM measurements (much more than the 3072 used in this investigation) are needed to overcome the

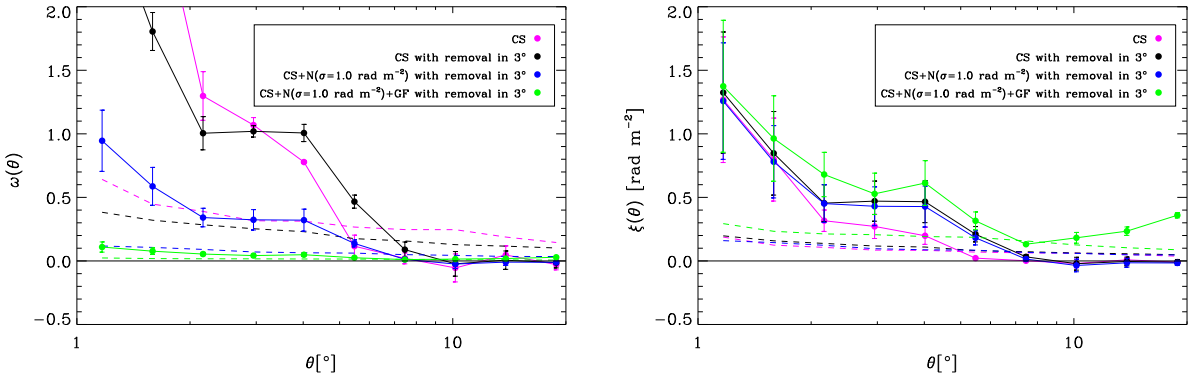

Figure 10. Changes in the cross-correlation functions for the two estimators ω_{RM} (left panel) and ξ_{RM} (right panel) when gradually including all described steps to the cosmological signal (CS) using the *MHD Gal* simulation with a*magnetic depth* of the universe of $z = 1.03$. GF and N stand for Galactic foreground and observational noise respectively.

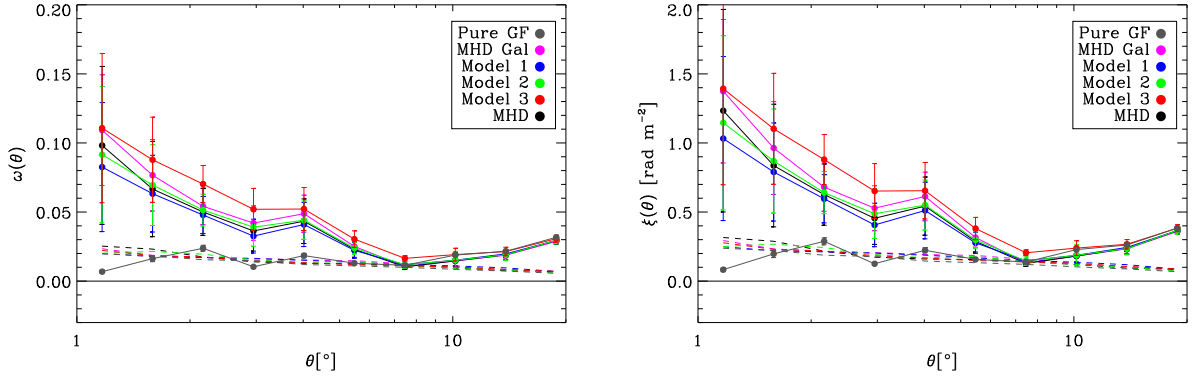

Figure 11. Cross-correlation functions for the different magnetic field models, using an optimistic *magnetic depth* for the cosmological signal (CS) (corresponding to a universe magnetized out to $z = 1.03$), taking into account the Galactic foreground (GF), assuming a Gaussian noise (N) with $\sigma_{\rm RM} = 1$ rad m^{-2} (as expected for the next generation of instruments) and applying the foreground subtraction in 3°. Left panel shows the result for normalized estimator ω_{RM} whereas the right panel shows the result for the unnormalized estimator ξ_{RM}.

statistical noise induced by the particular magnetic field realization within the cosmic structures, in order to distinguish between the wide range of models we used here. In general, the RM signal is strongly dominated by the denser regions (e.g. those populated by galaxy clusters and groups) and not by the low density ones, like filaments. On this point, the magnetic field associated with filaments already changes by several orders of magnitudes within the different models used here.

Aditionally, the normalized estimator ω_{RM} is extremely sensitive to measurement errors and to the presence of the GF (despite attempts to remove it by subtracting a smoothed map). It is fair to say that given the current measurement errors in the available RMs and our knowledge of the GF, present studies cannot determine the magnetization magnitude of the Universe based only on the cross-correlation ω_{RM}, whatever the significance of the measured signal is. On the contrary, the shape of the unnormalized estimator ξ_{RM} (the same as used by Lee et al. 2009) is relatively insensitive against the presence of measurement errors for the RMs and for the presence of the GF (as long as the described removal technique is used). Its amplitude, however, is quite strongly affected by measurement uncertainties. Current measurement errors (as for example those inherited by the Taylor's published sample) suppress the signal by a significant amount in such a way that it is impossible to relate the amplitude of the cross-correlation function to the underlying magnetization of the the large scale structure. However, we expect that future radio telescopes will be able of reaching error magnitudes of order of 1 rad m^{-2} that could make the correction of the signal possible.

Unfortunately, this estimator does not nicely encode in its shape the details of the magnetization of the large scale structure and, especially, its amplitude is extremely sensitive to the *magnetic depth* of the Universe. Therefore, any interpretation of an observed signal is limited by our knowledge of the redshift distribution of the sources (towards the RM signals measured), as well as by our knowledge of the distribution and evolution of the cosmic universal magnetization. Future observational data will help to put better constraints on theoretical models for the origin of cosmological magnetic fields which, in return, can be implemented in next generation of MHD cosmological simulations in order to draw a self-consistent picture that can be compared against observations.

In summary, we conclude that current RM observations cannot constrain the amplitude and distribution of magnetic fields within the large scale structure. On the other hand, future datasets, based on a larger number of observations with more accurate RMs, might

be able to shed light on the magnetic field distribution and evolution within these structures. However, very detailed model predictions are needed in order to compare with any observed cross-correlation signal. It will be a quite demanding task for future cosmological simulations to provide detailed enough information of the large scale structure magnetization process within a large enough volume to produce useful templates of such correlation functions which can then be compared directly to the observations.

ACKNOWLEDGEMENTS

The authors would like to thank André Waelkens for making the HAMMURABI code publicly available and for generating the RM synthetic map of the Galactic foregound. F. S. acknowledges partial support by PICT Max Planck 245 (2006) of the Ministry of Science and Technology (Argentina). S. E. N. acknowledges the support of the DAAD (Deutscher Akademischer Austausch Dienst). K. D. acknowledges the support of the DFG Priority Programme 1177.

REFERENCES

Adelman-McCarthy J. K., Agüeros M. A., Allam S. S., Allende Prieto C., Anderson K. S. J., Anderson S. F., Annis J., Bahcall N. A., Bailer-Jones C. A. L., Zucker D. B., 2008, ApJS, 175, 297

Beck R., 2009, Astrophysics and Space Sciences Transactions, 5, 43

Beck R., Gaensler B. M., 2004, New Astronomy Review, 48, 1289

Bonafede A., Feretti L., Murgia M., Govoni F., Giovannini G., Dallacasa D., Dolag K., Taylor G. B., 2010, arXiv:1002.0954

Dolag K., Grasso D., Springel V., Tkachev I., 2005, Journal of Cosmology and Astro-Particle Physics, 1, 9

Donnert J., Dolag K., Lesch H., Müller E., 2009, MNRAS, 392, 1008

Górski K. M., Hivon E., Banday A. J., Wandelt B. D., Hansen F. K., Reinecke M., Bartelmann M., 2005, ApJ, 622, 759

Govoni F., 2006, Astronomische Nachrichten, 327, 539

Han J. L., Manchester R. N., Lyne A. G., Qiao G. J., van Straten W., 2006, ApJ, 642, 868

Hoffman Y., Ribak E., 1991, ApJ, 380, L5

Jansson R., Farrar G. R., Waelkens A. H., et al. 2008, in International Cosmic Ray Conference Vol. 2 of International Cosmic Ray Conference, Large scale magnetic field of the Milky Way from WMAP3 data. pp 223–226

Lee J., Pen U., Taylor A. R., Stil J. M., Sunstrum C., 2009, arXiv:0906.1631

Mathis H., Lemson G., Springel V., Kauffmann G., White S. D. M., Eldar A., Dekel A., 2002, MNRAS, 333, 739

Nuza S. E., Dolag K., Saro A., 2010, submitted to MNRAS

Page L., Hinshaw G., Komatsu E., Nolta M. R., Spergel D. N., Bennett C. L., Barnes C., Bean R., Doré O., Dunkley J., Halpern M., Hill R. S., et al. 2007, ApJS, 170, 335

Sun X. H., Reich W., 2009, A&A, 507, 1087

Sun X. H., Reich W., Waelkens A., Enßlin T. A., 2008, A&A, 477, 573

Taylor A. R., Stil J. M., Sunstrum C., 2009, ApJ, 702, 1230

Waelkens A., Jaffe T., Reinecke M., Kitaura F. S., Enßlin T. A., 2009, A&A, 495, 697